Supporting Information

Wurster et al. 10.1073/pnas.1005507107

SI Text

Normal Alkanes. Normal alkanes (*n*-alkanes) are structurally the simplest class of lipids comprising saturated carbon atoms arranged as linear chains that can vary in length (homologs) but have the same empirical formula: C_nH_{n+2}. They constitute a major component of epicuticular waxes that are found on the leaves and stems of higher plants, where they serve as a protective layer to the plant preserving its water balance, minimizing mechanical damage to leaf cells, and inhibiting attack by fungi and invertebrates (1). Previous work has shown that the relative distribution of the *n*-alkane homologs in epicuticular waxes may be used to discriminate between different species of vegetation (2). The survival of *n*-alkanes in sediments and their use as indicators for determining the source of organic matter are already well-established (3–5). Furthermore, the recalcitrance of *n*-alkanes has already been exploited as a means of estimating the intake of vegetation by herbivores, where it survives passage through the gastrointestinal system to provide a biogeochemical signature of ingesta (6). This study exploits the *recalcitrance* and *chemotaxonomic utility* of *n*-alkane distributions.

Briefly, fauna inhabiting a cave will have ingested local vegetation and/or invertebrates that will have been feeding on local vegetation. Either way, the *n*-alkane component of the leaf epicuticular waxes will be preserved and deposited as cave guano, forming a record derived directly from and representative of local vegetation. Large shifts in previous vegetation may be represented by a shift in the relative distribution of *n*-alkane homologs; this explains the changes observed for the C_{29}/C_{31} *n*-alkane ratio. If the shift in vegetation results in a majority shift to a species that utilizes a different pathway for fixation of CO_2 (i.e., C_3 to C_4 and vice versa), then the observed distributional shift will be accompanied by a corresponding shift in the $\delta^{13}C$ value of the *n*-alkanes, as observed. It was determined that the $\delta^{13}C$ value of the weighted mean average of *n*-alkane distributions obtained from a variety of flora was depleted in $\delta^{13}C$, relative to total tissue, by an average of 7.6‰ (per mille) (7). However, more importantly, a large average difference of ~12‰ was observed for the *n*-alkane fractions derived from the C_3 and C_4 species and, crucially, it is this isotopic signature that is retained by the *n*-alkanes preserved in the cave guano deposits.

Estimation of C_4 Biomass Contribution. Precise determination of the abundance of C_4 biomass inferred from guano $\delta^{13}C$ values is not possible at this time due to a paucity of ground-truthing data, particularly for Southeast Asia. However, we compare two independent estimations of C_4 biomass to indicate a possible range in values: (*i*) empirically derived C_4 plant estimations determined from a study on insectivorous bat guano and (*ii*) assuming a simple mass balance model. Results are reported in Table S3.

Empirically derived estimates. An empirically derived equation for bat guano from the southwest United States has been published (8). C_4 plant relative abundance was determined using a spatially explicit model using latitude and longitude as inputs (9), and this was compared with $\delta^{13}C$ values of bulk guano to determine a strongly significant linear regression. We have modified this equation to assume that sites with less than 25 mm precipitation/y have no contribution of C_4 biomass (9). We also plot $\delta^{13}C$ values of insect cuticles to show that these values are similar to bulk guano, and these results are illustrated in Fig. S3.

Mass balance. It is possible to estimate the abundance of C_4 biomass assuming a simple mass balance model where

$$\delta^{13}C_{IC} = X \times (\delta^{13}C\text{-}C_4 + \varepsilon_4) + (1 - X) \times (\delta^{13}C\text{-}C_3 + \varepsilon_3),$$

where $\delta^{13}C_{IC}$ is the $\delta^{13}C$ value of insect cuticles (extracted from the cave guano), X is the proportion of C_4 biomass, $\delta^{13}C$-C_4 is the average $\delta^{13}C$ value of C_4 biomass, $\delta^{13}C$-C_3 is the average $\delta^{13}C$ value of C_3 biomass, and ε is the fractionation between dietary plant biomass and insect cuticles (which may be different between C_4 and C_3 vegetation). For a rough calculation under current atmospheric $\delta^{13}C$ values, C_4 biomass can be estimated to be −12.5‰ and C_3 can be estimated to be −27.5‰ for C_3 biomass (10–12). Under different atmospheric $\delta^{13}CO_2$ conditions, it is possible to compensate for changed plant endmember values by simply adding the difference to the insect cuticle $\delta^{13}C$ value. We take ε values from insects cultured on C_3 or C_4 biomass (13), where $\varepsilon_3 = 0.8$ and $\varepsilon_4 = 0$ (see refs. 14 and 15 for comparable values).

1. Eglinton G, Hamilton RJ (1967) Leaf epicuticular waxes. *Science* 156:1322–1335.
2. Del Castillo JB, et al. (1967) Taxonomic distribution of some hydrocarbons in gymnosperms. *Phytochemistry* 6:391–398.
3. Eglinton G, Scott PM, Belsky T, Burlingame AL, Calvin M (1964) Hydrocarbons of biological origin from a one-billion-year-old sediment. *Science* 145:263–264.
4. Thompson S, Eglinton G (1978) The fractionation of a recent sediment for organic geochemical analysis. *Geochim Cosmochim Acta* 42:199–207.
5. Huang YS, Lockheart MJ, Collister JW, Eglinton G (1995) Molecular and isotopic biogeochemistry of the Miocene Clarkia Formation: Hydrocarbons and alcohols. *Org Geochem* 23:785–801.
6. Dove H, Mayes RW (1991) The use of plant wax alkanes as marker substances in studies of the nutrition of herbivores: A review. *Aust J Agric Res* 42:913–952.
7. Collister JW, Rieley G, Stern B, Eglinton G, Fry B (1994) Compound-specific $\delta^{13}C$ analyses of leaf lipids from plants with differing carbon dioxide metabolisms. *Org Geochem* 21:619–627.
8. Wurster CM, McFarlane DA, Bird MI (2007) Spatial and temporal expression of vegetation and atmospheric variability from stable carbon and nitrogen isotope analysis of bat guano in the southern United States. *Geochim Cosmochim Acta* 71:3302–3310.
9. Paruelo JM, Lauenroth WK (1996) Relative abundance of plant functional types in grasslands and shrublands of North America. *Ecol Appl* 6:1212–1224.
10. Ehleringer JR, Cerling T (2002) In *Encyclopedia of Global Environmental Change*, eds Mooney HA, Gandadell JG (John Wiley & Sons, Chichester), pp 186–190.
11. Koch PL, Diffenbaugh NS, Hoppe KA (2004) The effects of late Quaternary climate and pCO_2 change on C_4 plant abundance in the south-central United States. *Palaeogeogr Palaeoclimatol Palaeoecol* 207:331–357.
12. Randerson JT, et al. (2005) Fire emissions from C_3 and C_4 vegetation and their influence on interannual variability of atmospheric CO_2 and $\delta^{13}CO_2$. *Global Biogeochem Cycles* 19:GB2019.
13. Gratton C, Forbes AE (2006) Changes in δ ^{13}C stable isotopes in multiple tissues of insect predators fed isotopically distinct prey. *Oecologia* 147:615–624.
14. Webb SC, Hedges REM, Simpson SJ (1998) Diet quality influences the $\delta^{13}C$ and $\delta^{15}N$ of locusts and their biochemical components. *J Exp Biol* 201:2903–2911.
15. Chamberlain PM, Bull ID, Black HI, Ineson P, Evershed RP (2004) Lipid content and carbon assimilation in Collembola: Implications for the use of compound-specific carbon isotope analysis in animal dietary studies. *Oecologia* 139:325–335.

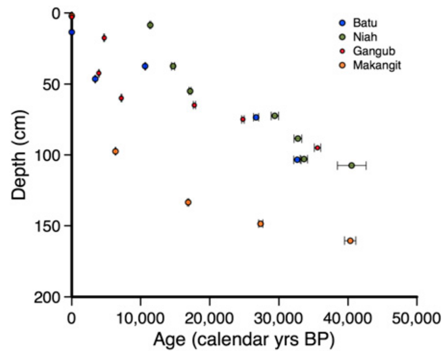

Fig. S1. Calibrated calendar years as a function of depth for the four guano profiles. Three total dates were considered to contain exogenous carbon and were not used in the age model.

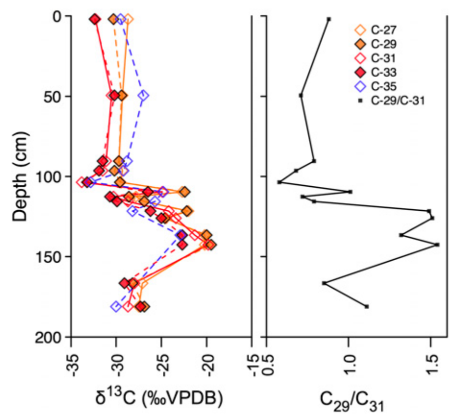

Fig. S2. $\delta^{13}C$ values of *n*-alkanes and C_{29}/C_{31} from the Makangit guano profile. Distinctly high $\delta^{13}C$ values covary with C_{29}/C_{31} and have been dated to the Last Glacial Maximum. These values can be attributed to a significant increase in C_4 biomass at that time.

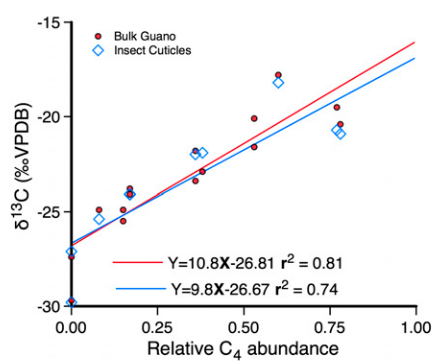

Fig. S3. $\delta^{13}C$ values of bat guano from the southwest United States as a function of estimated C_4 relative abundance as described in *SI Text*. Closed circles are from bulk guano samples and open diamonds are from processed insect cuticles.

Table S1. Radiocarbon dates on guano deposits from Batu, Niah, Gangub, and Makangit caves

Sample identifier*	Publication code	Conventional radiocarbon age (y BP $\pm 1\sigma$)	Calibrated calendar age (y BP $\pm 2\sigma$)
Batu			
Batu 12–15	SUERC-24432	Modern	Modern
Batu 36–39 (charcoal)	SUERC-20983	9,419 ± 43	10,651 ± 64
Batu 45–48†	SUERC-24433	3,193 ± 38	3,417 ± 37
Batu 72–75	SUERC-24434	22,196 ± 151	26,712 ± 365
Batu 101–105	SUERC-20987	28,367 ± 330	32,670 ± 528
Niah			
GU1 6–10	SUERC-20986	9,932 ± 44	11,359 ± 95
GU1 36–39	SUERC-20539	12,513 ± 51	14,673 ± 236
GU1 54–56	SUERC-20540	14,090 ± 60	17,155 ± 158
GU1 70–75 (SEG)	SUERC-6527	24,572 ± 491	29,418 ± 545
GU1 86–90	SUERC-24403	28,436 ± 333	32,769 ± 551
GU1 101–105	SUERC-20541	28,976 ± 351	33,630 ± 528
GU1 105–110 (SEG)	SUERC-6525	35,327 ± 1932	40,545 ± 2074
Gangub			
GAN1 0–7 FP	SUERC-17475	Modern	Modern
GAN1 15–20 FP	SUERC-20542	4,150	4,694 ± 77
GAN1 40–45 FP†	SUERC-17462	3,627	3,945 ± 58
GAN2 15–20 FP†	SUERC-20543	6,279	7,204 ± 59
GAN2 20–25	SUERC-24402	14,609	17,769 ± 154
GAN2 30–35 FP	SUERC-17464	20,797	24,778 ± 192
GAN2 55–60 (SEG)	SUERC-20993	30,926	35,593 ± 484
Makangit‡			
Ile2 1–3	SUERC-17466	Modern	Modern
Ile2 96–99	SUERC-21181	5,548 ± 53	6,348 ± 46
Ile2 132–135	SUERC-17470	13,768 ± 58	16,883 ± 87
Ile2 147–150	SUERC-20536	22,680 ± 162	27,375 ± 315
Ile-2 159–162	SUERC-20535	35,279 ± 779	40,325 ± 811

*All radiocarbon dating was performed on extracted insect cuticles unless otherwise noted. The sole charcoal sample was from handpicked in situ charcoal fragments. SEG, solvent-extracted guano with Acid-Base-Acid (ABA) treatment (1).
†Radiocarbon date was not used in determination of age model.
‡Makangit calibrations necessitated correction for the presence of lithogenic graphite.

Table S2. Corrections on radiocarbon measurements of Makangit samples due to the presence of lithogenic graphite

Sample identifier	Publication code	Graphite (%)	% modern ^{14}C	% modern ^{14}C corrected
Ile2 96–99	SUERC-21181	8	46.0 ± 0.33	50.1
Ile2 132–135	SUERC-17470	5	17.1 ± 0.13	18.0
Ile2 147–150	SUERC-20536	1	5.9 ± 0.12	5.9
Ile-2 159–162	SUERC-20535	3	1.2 ± 0.12	1.2

Graphite abundance was estimated by using a Philips PW1050/Hiltonbrooks DG2 X-ray diffractometer (XRD). Graphite has a distinct XRD peak at the 30.98 2θ lattice plane. Using differing weights of graphite, mixed with a chitin abundance standard (elemental microanalysis), a peak area/graphite abundance relationship was determined. The area under the graphite peak of density-separated samples was compared with this peak area/graphite relationship function to estimate graphite abundance of unknown samples. Corrected percent modern ^{14}C was determined assuming that lithogenic graphite contributed effectively ^{14}C-free carbon to the sample and a graphite corrected conventional radiocarbon age was determined.

Table S3. Inferred savanna production at Sundaland sites from the Last Glacial Maximum

	Modern			~10 kya			Last Glacial Maximum		
		Estimated C_4 production (%)			Estimated C_4 production (%)			Estimated C_4 production (%)	
Site	$\delta^{13}C$	(1)	(2)	$\delta^{13}C$	(1)	(2)	$\delta^{13}C$	(1)	(2)
Batu	−25.6	11	8	−25.7	0	0	−21.1	43	33
Niah	−26.7	2	0	−25.7	0	0	−26.0	0	0
Gangub	−24.7	19	14	−25.4	0	0	−18.1	69	54

$\delta^{13}C$ values are reported in per mille (‰) units normalized to VPDB. The C_4 production estimate is based on bat guano $\delta^{13}C$ values regressed against spatially estimated C_4 plant production in the southwest United States assuming sites with <25 mm precipitation/y had no C_4 production, or calculated as a simple mixing model using 100% C_3 as −27.5 and 100% C_4 as −12.5‰, and tissue fractionation between C_3 diet and tissue of 0.8‰, and 0‰ between C_4 diet and tissue. In all cases, insect cuticles were adjusted to compensate for changes of $\delta^{13}C$ values of atmospheric CO_2. See *SI Text* for details.